LASER ABLATION SYSTEM WITH A DIODE LASER FOR AMS ^{14}C MEASUREMENT OF ORGANIC MATERIALS

Fumina Minamitani[1]* • Takayuki Omori[2] • Kohei Yamazaki[2] • Hiromasa Ozaki[2] • Masataka Hakozaki[3] • Minoru Yoneda[2]

[1]Department of Integrated Biosciences, Graduate School of Frontier Sciences, The University of Tokyo 5-1-5, Kashiwanoha, Kashiwa, Chiba 277-8561, Japan
[2]Laboratory of Radiocarbon Dating, The University Museum, The University of Tokyo 7-3-1, Hongo, Bunkyo, Tokyo 113-003, Japan
[3]National Museum of Japanese History, 117 Jonai-cho, Sakura City, Chiba 285-8502, Japan

ABSTRACT. We constructed a laser ablation (LA) system using a diode laser for the accelerator mass spectrometry radiocarbon (AMS ^{14}C) measurement of organic materials. The system could extract adequate CO_2 to analyze small masses (0.1 mg C) at a resolution of 250 μm by a 5.5 W diode laser. The LA system was assessed using standard materials (IAEA-C1, IAEA-C2, IAEA-C3, IAEA-C6, and Ox II) and applied to natural tree ring samples. For the LA sampling of organic samples, which generally results in incomplete combustion, tungsten (VI) oxide was used as an oxidant to achieve complete burning. The results of the measurement of standard materials showed a low ^{14}C background of F^{14}C 0.0085 ± 0.0005 and reasonable reproduction of ^{14}C values. Finally, we applied this system to a single-year analysis of tree-ringed spruce timber in Alaska. It was observed to have a detectable background for the ^{14}C bomb peak.

KEYWORDS: diode laser, graphitization, laser ablation, organic materials, radiocarbon.

INTRODUCTION

The mapping of chemical compositions is an effective approach for revealing the chemical dynamics of biological tissues and sedimentological structures at a high resolution. The distribution of chemical compositions visualized by mapping is effective for understanding physiological phenomena and the biochemical processes in living organisms. It is used in a wide range of fields including medicine, environmental science, geochemistry, and archaeology. In recent years, high-resolution radiocarbon (^{14}C) measurements were realized through the development of sampling methods that utilize laser ablation (LA). This has yielded novel observations. The technique was developed primarily for inorganic materials. Many studies on stalagmite, coral, and shell samples have been reported. For example, Andrews et al. (2019) investigated a continuous record of ^{14}C uptake in the growth layers of red snapper otoliths and demonstrated a 60-year longevity for the red snapper. Welte et al. (2021) analyzed radiocarbon and stable carbon isotopes in stalagmite samples at a resolution of 100 μm. They showed that the carbon isotope dynamics correlated with the past climate changes in karst systems.

In a pioneering study, Rosenheim et al. (2008) developed laser ablation-accelerator mass spectrometry (LA-AMS) based on LA-ICP-MS. They performed high-spatial-resolution analysis of radiocarbon measurements. This system consists of a large laser system (Nd:YAG 213 nm laser) and a sample chamber filled with carrier gas. It has become the standard setup for high-resolution analysis because it can efficiently generate CO_2 from the surface of carbonates. Subsequently, the development of the LA-AMS was considered for optimizing the design of the LA sampler, type of laser head, and adjustment to the AMS gaseous ion source (Welte et al.

*Corresponding author. Email: minamitani-fumina783@g.ecc.u-tokyo.ac.jp

2016a, 2016b, 2017). Kitagawa (2013) proposed an LA method using a smaller 30 W CO_2 laser with a vacuum chamber only for CO_2 production followed by graphitization. It showed a low background comparable to that of conventional carbonates preparation.

In this historical context, there have been few practical applications of LA for the radiocarbon measurement of organic materials. However, LA has the potential for application to organic materials if it is used as a pretreatment for graphitization, rather than using LA-(gas ion source)-AMS (which requires the instantaneous generation of a large amount of CO_2). A typical LA-ICP-MS has a large amount of energy (several tens of watts) to instantaneously introduce evaporated and particulate samples into the ion source (Günther and Heinrich 2002; Prohaska et al. 2016). Meanwhile, the AMS method using a solid target requires at most 50 μg of carbon (Hua et al. 2004). That is, in developing a pretreatment system for AMS by graphitization, it is likely that a small laser with an output of at most 10 W can be applied effectively by irradiation for a long period of time (a few seconds). This is because it only needs to increase the temperature of a small sample and generate CO_2 by LA. If LA-graphitization can be realized by combining the existing solid-ion-source AMS with a conveniently available laser, it can be applied actively to a wide range of organic materials (such as teeth, bones, and tree rings) in a wide range of fields including biology and medicine.

This study aimed to develop an LA system for organic materials using a readily available diode laser. First, we analyzed the characteristics and specifications of the laser using inorganic materials as reference materials by comparing several parameters. Then, we evaluated the differences between these and the LA characteristics observed when applied to organic materials. Second, we detected the bomb peak using a tree ring and discussed the feature applications of the LA system.

LASER SAMPLING SYSTEM

The sampling system consisted of a consumer diode laser and a sample chamber on a three-axis (XYZ) stage that could adjust the sample position with an accuracy of 0.01 mm (Figure 1). CO_2 was purified cryogenically from the produced gas and reduced to graphite in a separated sealed tube using conventional sample preparation methods (Kitagawa et al. 1993). The ^{14}C concentration was then measured using an accelerator mass spectrometer.

A laser diode (NEJE, N30820™) with a maximum output of 5.5 W was installed in the system with the following settings: emission wavelength near 450 nm, operation in continuous-wave oscillation mode, and compact specifications (30 × 30 × 110 mm, 202 g). It is generally used for laser cutting and laser engraving of wood and plastic. A single-board microcontroller (Arduino UNO™) controlled the output (%) and irradiation time (ms/shot). The laser output could be varied 0-100 % in 3.3-12 V of PWM control. The system was equipped with a CCD camera to capture images of the sample surface during the LA. The sample chamber can hold samples with maximum diameter and height of 35 mm and 14 mm, respectively. It was equipped with a three-axis stage with an accuracy of 0.01 mm and a travel of ±6.5 mm in the XY axis in the horizontal plane. After placing the sample, the chamber was sealed with soda-lime glass and an O-ring. Because the residual atmospheric gases in the chamber that do not originate from the sample can cause a high background, the chamber was evacuated for approximately 30 min prior to LA (decompression to approximately 1/100,000 atm). After LA, the pressure increased as the sample produced a mixture of carbon dioxide, water, and nitrogen oxide gases. Carbon
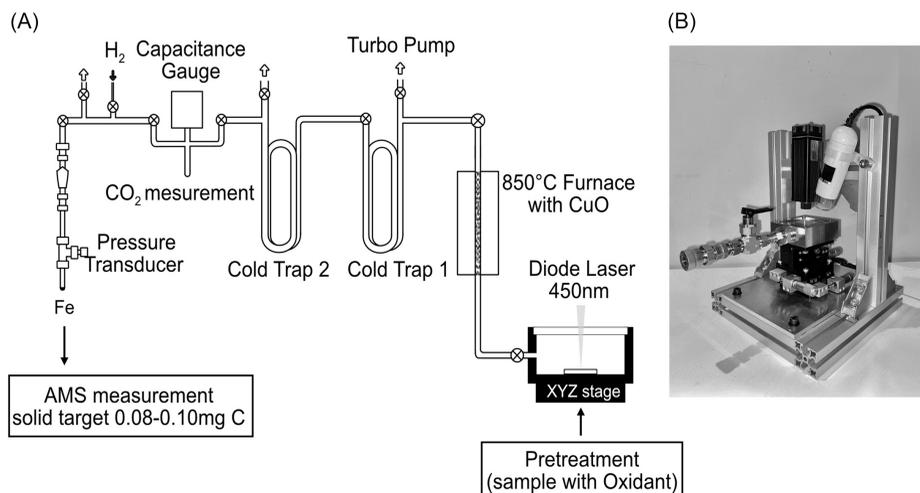
Figure 1   Schematic of the system (A) and photograph of the laser ablation unit (B). The samples are mixed with an oxidant and placed in the LA-cell. After passing through a furnace filled with copper oxide (850°C), the gas produced by LA is purified of carbon dioxide with a refrigerant, which is quantified with a capacitance gauge as an AMS target. The measurements are performed with a Compact AMS (0.5MV 105SDH-1).

dioxide was separated from the mixed gas in a vacuum glass line and reduced with hydrogen to prepare graphite.

MATERIALS

The standards used in the experiments described below are listed in Table 1 (Rozanski et al. 1992). IAEA C1 (marble) and C2 (travertine), which are fragmented carbonates, were powdered with a ceramic motor. IAEA C3 is a 1 mm thick cellulose sheet. Granular IAEA C6 (sucrose), NIST Ox II (oxalic acid) and our laboratory blank (oxalic acid, Wako Chemical) were also powdered with a ceramic motor.

The growth rings in a piece of Sitka spruce (*Picea sitchensis*) wood from Alaska, U.S.A. were measured for the radiocarbon abundance. The sample was dated rigorously to AD 1689–1990 by dendrochronology (Hakozaki and Nakamura 2013). Twelve annual rings from AD 1950 to AD 1983 were analyzed.

METHODS

Laser Ablation Sampling

CO_2 was produced by LA in a vacuum chamber after pretreatment depending on the shape and type of the sample. The sample was placed on a thin aluminum disk at the inner bottom of the sample chamber to prevent contamination from the stainless steel. The samples were powdered using a ceramic motor and the homogenized. For certain samples, an oxidant (tungsten (VI) oxide; Elementar, S11.02-0008) was added to achieve complete combustion. Tungsten oxide is used as an additive in elemental analysis, has a higher heat capacity than other oxidants such as copper oxide, and generates a large amount of thermal energy. Given the inherent complexities in utilizing gaseous oxygen as a supply source (including the need for precise volumetric control

Table 1 Overview of the different materials used for LA-AMS and comparison of the CO_2 production with and without an oxidant.

Sample name	Material	Laser shot time (ms)	Without oxidant			With oxidant		
			µgC/spot	1SD	N	µgC/spot	1SD	N
C1	Marble	200	7.7	2.5	3	17.4	2.1	9
C2	Travertine	250–300	18	3.2	4	16.1	2.2	11
C3	Cellulose	200–300	4.2	1	15	23.6	9.7	8
C6	Sucrose	1000–2000	0.3	0.3	5	15.8	4.6	4
OxII (SRM-4990c)	Oxalic acid	200–300	0.5	0.3	10	20.3	2.9	10

and the use of high-purity cylinders), we employed a simpler method of oxygenation by incorporating powdered tungsten oxide into the sample. The oxidant was ground using a ceramic motor and sieved through a mesh (212 µm mesh aperture). The powdered sample and oxidant were homogenized and pressed into a steel mold (ϕ5 mm, thickness = 0.8 mm) using a hydraulic press at a press pressure of ca. 0.5 ton. It was then placed in the center of a laser ablation sampler.

After subjecting the sample to the preliminary treatment, it was placed within the chamber. The stage was adjusted precisely along the vertical Z-axis to align the laser focus to a diameter of 0.25 mm. The laser output and irradiation duration were varied systematically during the experiments. After the atmosphere in the chamber was fully evacuated, the valve of the chamber was sealed, and LA was performed.

Radiocarbon Analysis

The CO_2 produced by LA accumulated in the vacuum glass line system. This resulting in a total carbon quantity of 0.1 mg. Conventional radiocarbon measurements using AMS generally require 1 mg of carbon. Meanwhile, this study used the submicrogram measurements. Given that the gas produced by LA sampling could contain carbon monoxide resulting from the incomplete combustion of the sample, it was passed through a furnace at 850ºC. Herein, copper oxide converted CO to CO_2. The CO_2 was extracted cryogenically using liquid nitrogen (ca. –196ºC) and cooled ethanol (at approximately –90ºC), and quantified with a capacitance gauge. Purified CO_2 was then mixed with two times the amount of H_2 and sealed within a 2-mL reaction-tube containing approximately 4 mg of reduced iron catalyst. The reaction tube was heated at 460ºC for 10 hr. The CO_2 was reduced to graphite at the surface of the iron powder. The final amount of analyzed carbon was calculated based on the internal pressure of the reaction vessel (Freeman et al. 2016).

AMS radiocarbon measurements were performed using a Compact AMS system (0.5 MV 1.5SDH-1, National Electrostatics Co.) at Laboratory of Radiocarbon Dating (LRD.UMUT), the University Museum, the University of Tokyo. The NIST oxalic acid (OxII) standard (SRM-4990c) was pretreated by LA. It was used for normalizing and correcting isotopic fractionation. The IAEA-C6 standards were used for batch-to-batch validation. The radiocarbon measurements were obtained using background correction and isotope fractionation correction with $\delta^{13}C$ based directly on AMS measurements (Stuiver and Polach 1977).
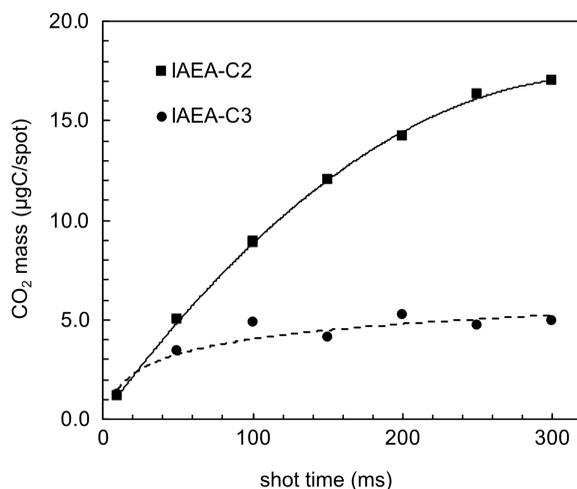
Figure 2   Comparison of carbon dioxide production between carbonate C2 and cellulose C3. The horizontal axis represents the time (msec) for which the laser is irradiated on a spot. The solid and dashed lines are the approximation curves.

RESULTS AND DISCUSSION

Production of Carbon Dioxide

First, the reproducibility of the CO_2 production and ^{14}C abundance was investigated using reference materials (Table 2). Carbonates (ex. IAEA-C2) efficiently produced carbon dioxide through thermal decomposition, whereas organic materials such as cellulose (ex. IAEA-C3) did not produce significant quantities of CO_2 without oxidants. This indicated an incomplete combustion owing to their low oxygen content (Figure 2). The amount of CO_2 produced by LA varied significantly across samples. There were classified into three categories. In the case of IAEA-C2, a temporally linear increase in the amount of CO_2 produced was observed, and CO_2 corresponding to 17.0 µg C was produced from a spot at 300 ms. Meanwhile, IAEA-C3 produced less (at most 5.2 µg C, one-third the amount of C2), and IAEA-C6 and HOxII did not yield CO_2.

The addition of tungsten oxide significantly increased the production of IAEA-C6 to 15.8 µg C (at a shot time of 1000–2000 ms) and that of HOxII to 20.3 µg C (at a shot time of 200–300 ms). This could have been caused by an efficient combustion through the supply of oxygen to the organic materials. In such cases, the addition of tungsten oxide promotes complete combustion and increases the amount of carbon dioxide generated. The amount recovered was also increased in most cases in the presence of the oxidant. LA of organic materials requires the adjustment of the optimal combustion method according to the characteristics of each sample.

Background Level

The effect of tungsten oxide contamination was evaluated by comparing the results of IAEA-C1 in the presence and absence of tungsten oxide. IAEA-C1 displayed a $^{14}C/^{12}C$ of 1.21×10^{-14} ± 7.20×10^{-15} without tungsten oxide and of 1.27×10^{-14} ± 3.05×10^{-15} with tungsten oxide. There were marginally higher in the presence of tungsten oxide. Notably, the $^{14}C/^{12}C$ of blank

Table 2 Measurement results obtained by LA analysis and the consensus values.

Sample type	Laser power (%)	Shot time/spot (ms)	Carbon weight (mgC)	^{12}C current (µA)	Count rate (cpm)	$F^{14}C$
C1[a]						0.0000 ± 0.0002[a]
	50	500	0.157	2.9	5	0.0098 ± 0.0006
	50	500	0.167	2.5	4	0.0085 ± 0.0005
	50	500	0.084	4.8	16	0.0166 ± 0.0014
	50	500	0.124	2.8	7	0.0124 ± 0.0001
	50	500	0.119	5.2	10	0.0099 ± 0.0001
C2[a]						0.4114 ± 0.0003[a]
	100	300	0.141	4.2	329	0.4245 ± 0.0049
	100	300	0.116	2.1	169	0.4253 ± 0.0042
	100	300	0.114	1.6	127	0.4279 ± 0.0050
	100	300	0.117	1.9	156	0.4250 ± 0.0044
	100	300	0.111	4.0	327	0.4199 ± 0.0029
Oxalic acid (^{14}C free)						0.0000 ± 0.0000
	100	300	0.145	4.0	0	0.0083 ± 0.0031
	100	300	0.115	7.1	7	0.0083 ± 0.0015
	100	300	0.116	19.1	40	0.0114 ± 0.0031
	100	300	0.111	5.6	6	0.0063 ± 0.0007
C3[a]						1.2941 ± 0.0006[a]
	100	300	0.138	4.5	1033	1.3084 ± 0.0097
	100	300	0.134	1.4	333	1.3102 ± 0.0122
	100	300	0.144	6.3	1493	1.3149 ± 0.0094
	100	300	0.114	6.3	1486	1.2911 ± 0.0045
	100	300	0.117	3.2	750	1.2948 ± 0.0065
C6[a]						1.5061 ± 0.0011[a]
	100	2000	0.156	12.3	3385	1.5242 ± 0.0036
	100	2000	0.188	12.0	3238	1.5212 ± 0.0033
	100	2000	0.115	16.1	4628	1.5007 ± 0.0073
	100	2000	0.118	4.7	1314	1.4925 ± 0.0054
	100	2000	0.117	5.5	1522	1.4973 ± 0.0052

[a]Consensus value: Rozanski et al. (1992).
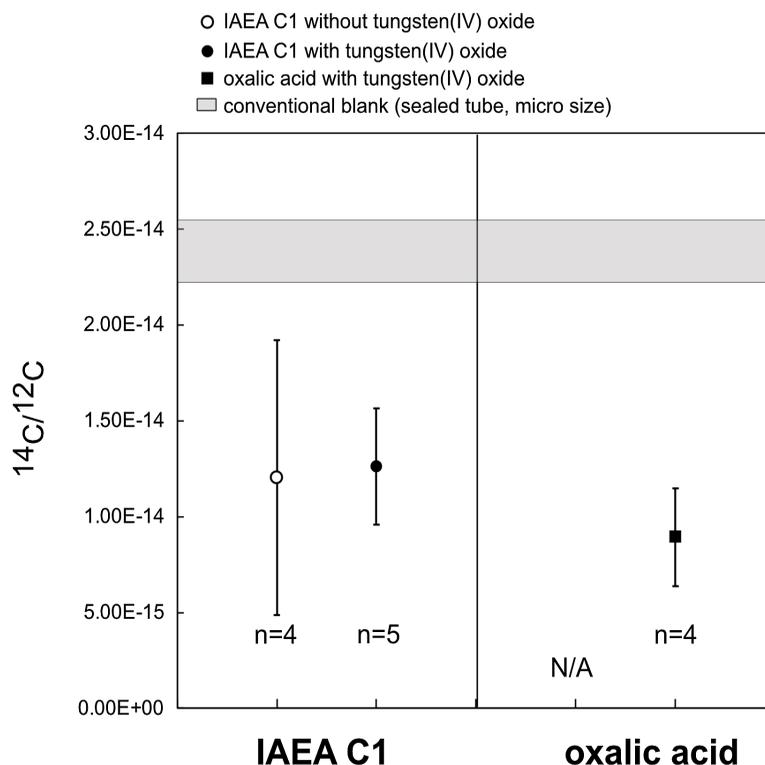
Figure 3   Effect of contamination by an oxidant (circles) of IAEA C1 and the blank level of the LA system with oxalic acid (^{14}C free) (squares). The open symbols are for combustion without tungsten oxide, and the solid symbols are for $^{14}C/^{12}C$ when combusted with tungsten oxide. The data for oxalic acid without tungsten oxide are not shown because the amount of CO_2 generated was insufficient. The shading indicates oxalic acid (n = 1) obtained by the conventional method (sealed tube combustion, 0.1 mg of carbon). These are not corrected for the background and $\delta^{13}C$.

oxalic acid with tungsten oxide was observed to be the lowest at $8.94 \times 10^{-15} \pm 2.57 \times 10^{-15}$. These blank levels associated with the LA system were sufficiently below the value of the blank obtained using the sealing method, which is considered a practical level.

Oxalic acid was used as a blank sample for organic matter. It cannot produce carbon dioxide without an oxidant. Therefore, the results obtained when the oxidant was added are shown (Figure 3). For a comparison with conventional methods, the results of small-mass measurements of blank oxalic acid using the sealing method over the past year are shown (Figure 3).

AMS ^{14}C Measurement of Standards

To ascertain the validity of carbon dioxide produced by LA for ^{14}C analysis, four IAEA-C series were used to perform ^{14}C measurements on the LA system. The standard samples were C1 (marble) and C2 (travertine) carbonates, oxalic acid for background measurement, and C3 (cellulose) and C6 (sucrose) organic materials. Tungsten oxide was added to all the standard samples. The consensus values were replicated without complexities. This indicated that the system was sufficiently functional (Table 2). The mean value of C1 was F^{14}C 0.0114 ± 0.0032,
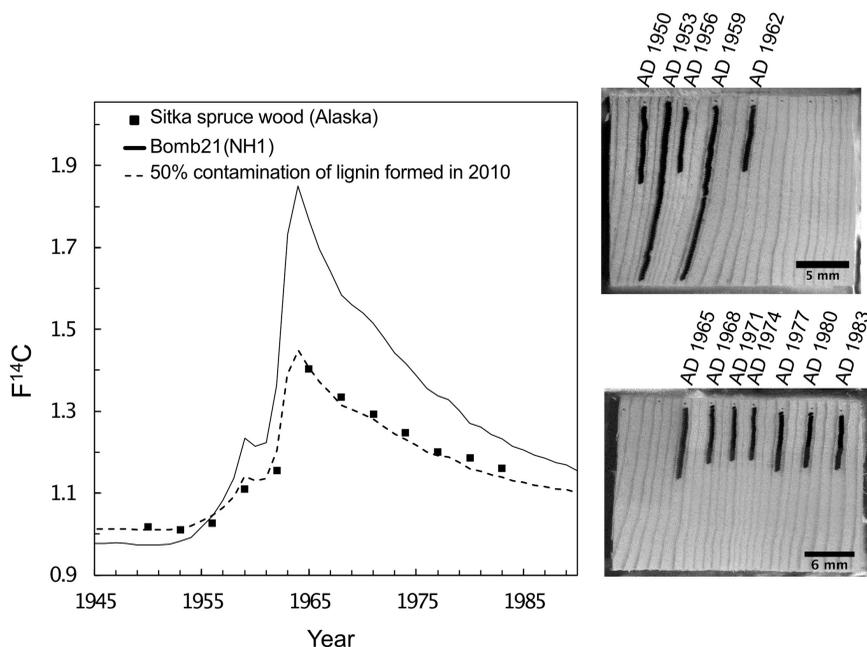
Figure 4 ^{14}C concentrations and Bomb 21(NH1) for 12 points from AD 1950 to 1983 obtained from Alaska Sitka spruce. The dashed line is the value when Bomb 21(NH1) is mixed with 50% of the 2010 ^{14}C value (the year the sample was harvested). The photograph on the right in Figure 4 shows the laser irradiation marks on each annual ring.

and that of C2 was F^{14}C 0.4245 ± 0.0029. These agreed with the consensus value of F^{14}C 0.4114 ± 0.0003. The mean value of the blank oxalic acid for the organic materials was F^{14}C 0.0908 ± 0.1840. The mean values of C3 (F^{14}C 1.3039 ± 0.0103) and C6 (F^{14}C 1.5072 ± 0.0145) agreed with the consensus values of F^{14}C 1.2941 ± 0.0006 and F^{14}C 1.5061 ± 0.0006, respectively.

Tree Rings

A rapid preparation with LA can accelerate the analysis of annual tree rings, for example, in the search for cosmic ray events. To validate the analysis of tree rings using LA, Alaskan Sitka spruce grown in the mid-20th century was applied to the LA system. The period including the entire the bomb peak from AD 1950–1983 was studied and analyzed every three years for 12 points in individual annual rings. The wood was divided into two pieces because the total length (38 mm) exceeded the chamber size. The spatial resolution was 250 μm horizontally and 490 μm vertically at each spot. Cellulose extraction was not performed, and no oxidate was added for a higher spatial resolution.

The LA-prepared samples showed a peak in AD 1965 that was parallel to the peak of Bomb21 (NH zone 1)(Hua et al. 2022; Figure 4; Table S1). The values of the pre-peak were marginally higher than those of Bomb21 (NH1), but those of post-peak were lower. Because wood was analyzed without chemical treatment, the effect of intermigratory substances such as lignin may have affected these results (Loader et al. 2003). Given that half of the total carbon originated from intermigratory subsistence, this lower peak could be simulated. The simulated

results obtained by assuming 2010 as the year of felling and intermigratory subsistence with an $F^{14}C$ of 1.0470 contributing half of the carbon in all the rings of the wood with the $F^{14}C$ values equivalent to Bomb21 (NH1) are shown by the dashed line in Figure 4. This result is in good agreement with our measurements using LA preparation. Coniferous wood contains 24–34% lignin and 15–20% hemicellulose (Silva et al. 1999; Hoch 2007). Therefore, the value used in the simulation (50%) was reasonable for their combined content.

CONCLUSION

Combining a solid-ion-source AMS and conveniently available 5.5 W diode laser, we constructed a laser ablation (LA) system that can be applied to organic materials. Organic matter with a low oxygen content was generally less likely to produce an amount of carbon dioxide equal to that produced by LA, than carbonates. However, complete combustion was promoted by the addition of an oxidant to the sample. The background signal was significantly lower than that observed with the conventional method. The consensus values for the certified reference materials were reproduced reasonably. When applied to the tree rings, the bomb peak was detected in good agreement with the simulated lignin and hemicellulose contents. The LA-^{14}C system can also be applied to organic materials. It is likely to be used for the rapid analysis of tree rings and ^{14}C mapping of biological tissues such as bones and teeth.

ACKNOWLEDGMENTS

SUPPLEMENTARY MATERIAL

To view supplementary material for this article, please visit https://doi.org/10.1017/RDC. 2023.71

REFERENCES

Andrews AH, Yeman C, Welte C, Hattendorf B, Wacker L, Christl M. 2019. Laser ablation–accelerator mass spectrometry reveals complete bomb ^{14}C signal in an otolith with confirmation of 60-year longevity for red snapper (*Lutjanus campechanus*). Marine and Freshwater Research 70:1768. https://doi.org/10.1071/MF18265

Freeman E, Skinner LC, Reimer R, Scrivner A, Fallon S. 2016. graphitization of small carbonate samples for paleoceanographic research at the Godwin Radiocarbon Laboratory, University of Cambridge. Radiocarbon 58:89–97. https://doi.org/10.1017/RDC.2015.8

Günther D, Heinrich CA. 2002. Enhanced sensitivity in laser ablation-ICP mass spectrometry using helium–argon mixtures as aerosol carrier† Plenary Lecture. Journal of Analytical Atomic Spectrometry 17:887–891. https://doi.org/10.1039/A901648A

Hakozaki M, Nakamura T. 2013. Tree-ring dating and dendroprovenancing of the imported Spruce woods. Departmental bulletin paper. https://doi.org/10.18999/bulnum.029.01

Hoch G. 2007. Cell wall hemicelluloses as mobile carbon stores in non-reproductive plant tissues. Functional Ecololgy 21:823–834. https://doi.org/10.1111/j.1365-2435.2007.01305.x

Hua Q, Turnbull JC, Santos GM, Rakowski AZ, Ancapichún S, De Pol-Holz R, Hammer S, Lehman SJ, Levin I, Miller JB, Palmer JG, Turney CSM. 2022. Atmospheric radiocarbon for the period 1950–2019. Radiocarbon 64:723–745. https://doi.org/10.1017/RDC.2021.95

Hua Q, Zoppi U, Williams AA, Smith AM. 2004. Small-mass AMS radiocarbon analysis at ANTARES. Nuclear Instruments and Methods in Physics Research B 223–224:284–292. https://doi.org/10.1016/j.nimb.2004.04.057

Kitagawa H. 2013. CO_2-laser decomposition method of carbonate for AMS ^{14}C measurements. Nuclear Instruments and Methods in Physics Research B 294: 218–220. https://doi.org/10.1016/j.nimb.2012.08.052

Kitagawa H, Masuzawa T, Makamura T, Matsumoto E. 1993. A batch preparation method for graphite targets with low background for AMS ^{14}C measurements. Radiocarbon 35:295–300. https://doi.org/10.1017/S0033822200064973

Loader NJ, Robertson I, McCarroll D. 2003. Comparison of stable carbon isotope ratios in the whole wood, cellulose and lignin of oak tree-rings. Palaeogeography, Palaeoclimatology, Palaeoecology 196:395–407. https://doi.org/10.1016/S0031-0182(03)00466-8

Prohaska T, Irrgeher J, Zitek A. 2016. Simultaneous multi-element and isotope ratio imaging of fish otoliths by laser ablation split stream ICP-MS/MC ICP-MS. Journal of Analytical Atomic Spectrometry 31:1612–1621. https://doi.org/10.1039/C6JA00087H

Rosenheim BE, Thorrold SR, Roberts ML. 2008. Accelerator mass spectrometry ^{14}C determination in CO_2 produced from laser decomposition of aragonite. Rapid Communications in Mass Spectrometry 22:3443–3449. https://doi.org/10.1002/rcm.3745

Rozanski K, Stichler W, Gonfiantini R, Scott EM, Beukens RP, Kromer B, van der Plicht J. 1992. The IAEA ^{14}C Intercomparison Exercise 1990. Radiocarbon 34:506–519. https://doi.org/10.1017/S0033822200063761

Silva JC, Nielsen BH, Rodrigues J, Pereira H, Wellendorf H. 1999. Rapid determination of the lignin content in Sitka Spruce (*Picea sitchensis* (Bong.) Carr.) wood by Fourier transform infrared spectrometry. Holzforschung 53:597–602. https://doi.org/10.1515/HF.1999.099

Stuiver M, Polach HA. 1977. Discussion: reporting of ^{14}C data. Radiocarbon 19:355–363. https://doi.org/10.1017/S0033822200003672

Welte C, Fohlmeister J, Wertnik M, Wacker L, Hattendorf B, Eglinton TI, Spötl C. 2021. Climatic variations during the Holocene inferred from radiocarbon and stable carbon isotopes in speleothems from a high-alpine cave. Climate of the Past 17:2165–2177. https://doi.org/10.5194/cp-17-2165-2021

Welte C, Wacker L, Hattendorf B, Christl M, Fohlmeister J, Breitenbach SFM, Robinson LF, Andrews AH, Freiwald A, Farmer JR, Yeman C, Synal H-A, Günther D. 2016a. Laser ablation – accelerator mass spectrometry: an approach for rapid radiocarbon analyses of carbonate archives at high spatial resolution. Analytical Chemistry 88:8570–8576. https://doi.org/10.1021/acs.analchem.6b01659

Welte C, Wacker L, Hattendorf B, Christl M, Koch J, Synal H-A, Günther D. 2016b. Novel laser ablation sampling device for the rapid radiocarbon analysis of carbonate samples by accelerator mass spectrometry. Radiocarbon 58:419–435. https://doi.org/10.1017/RDC.2016.6

Welte C, Wacker L, Hattendorf B, Christl M, Koch J, Yeman C, Breitenbach SFM, Synal H-A, Günther D. 2017. Optimizing the analyte introduction for ^{14}C laser ablation-AMS. Journal of Analytical Atomic Spectrometry 32:1813–1819. https://doi.org/10.1039/C7JA00118E